

Charged Higgs Bosons in non-minimal Supersymmetry

$A^0 \rightarrow H^\pm W^\mp$ in the λ SUSY-model at LHC

Glenn Wouda
Department of Physics and Astronomy,
Uppsala University

Degree Project D in Physics, 1FA597
Supervisor: Rikard Enberg

October 13, 2009

Abstract

In this thesis, we examine the Higgs-sector of the λ SUSY model and perform a benchmark study for $H^\pm \rightarrow h^0 W^\pm$ in $gg \rightarrow A^0 \rightarrow H^\pm W^\mp$ at the CERN LHC. The λ SUSY model is a version of NMSSM with a large coupling constant λ , which allows in particular the SM-like Higgs-boson to be substantially more massive than in e.g. the MSSM. We work in the approximation where the gauge-terms are neglected in the superpotential and the Higgs singlet S does not mix with the \mathcal{CP} -even states h^0, H^0 . What is left is a two-Higgs-doublet model and we evaluate Branching Ratios for the most important Higgs-decays using 2HDMC – a calculator for two-Higgs-doublet models. Total cross sections for different final states concerning the H^\pm in $gg \rightarrow A^0$ are obtained using `Pythia`.

We study the possibility to detect the H^\pm in $A^0 \rightarrow H^\pm W^\mp, H^\pm \rightarrow h^0 W^\pm \rightarrow VVW^\pm \rightarrow 4j W^\pm$ where there is one leptonic and one hadronic W -decay. The signal is generated with `Pythia v.8` and the background $pp \rightarrow t\bar{t} 2j$ in `MadGraph/MadEvent` and `Pythia`. With the analysis performed here, the signal is overwhelmed by the background, for the point in $(m_{H^\pm}, \tan\beta)$ -space we considered. The conclusion is that this signal is overwhelmed by the $t\bar{t} 2j$ background with this analysis.

We also study the $H^\pm \rightarrow t\bar{b}/\bar{t}b$ with the background $pp \rightarrow t\bar{t}$ for a point in the $(m_{H^\pm}, \tan\beta)$ -space with `Pythia`. We evaluated the invariant mass spectrum of $4j$ for signal and $t\bar{t}$ with the almost no further cuts. The conclusion is that the signal to background ratio is around 10^{-2} , and it might be difficult to improve the analysis to reach the desired level of background suppression

Populärvetenskaplig sammanfattning på Svenska

Denna uppsats behandlar fenomenologi hos supersymmetriska Higgs-partiklar. Den fysikaliska världen är uppdelad i två sorters partiklar; fermioner och utbytespartiklar. Varje fysikalisk kraft har sina egna, unika, utbytespartiklar. Det paradigm man har haft länge kallas Standardmodellen och inkluderar tre av de fyra kända krafterna. Teoretiskt sett så måste alla utbytespartiklar vara masslösa, men man har funnit i experiment att en viss sorts utbytespartiklar väger ungefär lika mycket som en järnatom. Detta problem löste man teoretiskt på 1960-talet i och med Higgsmekanismen, där man får ytterligare en partikel, Higgs-partikeln, samt genererar massor utbytespartiklarna. Alla sökningar efter Higgs-partikeln har misslyckats och man hoppas att CERNs nya experiment LHC kommer att finna experimentella evidens för dess existens.

Det finns idag en uppsjö indikationer på att standardmodellen måste utökas eller revideras. Två av de viktigaste orsakerna är existensen av mörk materia, vilket standardmodellen verkar sakna förklaring till. Den andra indikationen är att det verkar vara omöjligt att förena de tre krafterna som standardmodellen behandlar (elektromagnetism, starka kraften och svaga kraften). Styrkan på krafter beror på vilken energiskala man befinner sig på, detta är ett kvantmekaniskt fenomen som är väl dokumenterat experimentellt. Man har lyckats förena den svaga kraften med den elektromagnetiska, men ytterligare förening verkar omöjlig i standardmodellen. Vad man har funnit är att om man inkluderar något som kallas supersymmetri i standardmodellen så får man fler partiklar, varav några kan bidra till den mörka materian. Man finner även att förening av krafter är möjligt. Supersymmetri manifesterar sig i en relation mellan spinn hos olika partiklar. Spinn är den kvantmekaniska analogin med att en fast kropp roterar kring sin egen axel. Supersymmetri relaterar partiklar med olika spin med varandra, så att t.ex. elektronen, som har spinn $1/2$, har en supersymmetrisk partner med spinn 1 .

Man har alltså inte hittat higgs-partikeln, man har bara en undre gräns för dess massa. Därför har man formulerat en supersymmetrisk partikelmodell där man kan ha relativt tunga higgs-partiklar, konsistent med alla teoretiska och experimentella detaljer. Man har dock ett bivillkor som lyder att denna teori bara är giltig upp till en viss energiskala. När vi går över denna skala så bör vi se nya strukturer. I supersymmetri så får man flera stycken olika higgs-partiklar, varav två är elektriskt laddade. I projektet som ligger till grund för denna uppsats har vi tittat på några scenarier i denna modell, specifikt på om och hur man kan detektera de laddade higgs-partiklarna vid CERNs LHC. Metoden för detta är att skriva och använda datorprogram som simulerar vad som kan komma att hända vid LHC. Man producerar dessa higgs-partiklarna, och mycket mycket annat, i proton-proton kollisioner. I varje kollision bildas det flera tusen partiklar så det man som partikel-fenomenolog vill undersöka är om man kan hitta någon kvantitet som kan urskilja sig från det brus som uppstår.

Vi har här undersökt några punkter i parameterutrymmet för två sönderfallsprocesser hos den laddade higgs-partikeln. I båda fallen har de möjliga bakgrunderna översvämmat signalen

och det kommer vara omöjligt att se experimentella evidens för den laddade higgs om man använder sig av en liknande analys som vi har gjort här. Utsiktarna för denna supersymmetrisk modell är att ta reda på om det finns något sätt att förbättra analysen. Kanske kan man finna någon variabel som kan trycka ned bakgrunden med en faktor hundra?

Table of contents

1	Introduction	5
1.1	The Higgs boson in the Standard Model	5
1.2	Why extend the Standard Model?	7
1.3	Supersymmetry in Particle Physics	8
1.3.1	The Supersymmetry	8
1.3.2	Supersymmetric Higgs bosons	10
1.4	Why Supersymmetry?	12
1.5	Outline	13
2	The λSUSY model	14
2.1	Motivation	14
2.2	Higgs Sector	14
2.2.1	Mass Relations	14
2.2.2	Phenomenology of the λ SUSY Higgs sector within the 2HDM.	15
3	Benchmark point studies	21
3.1	Event Generation	21
3.2	Pythia Event Generator	21
3.3	MadGraph/MadEvent	22
3.4	Resonant Higgs production via Gluon fusion in pp -collisions	23
3.5	The process $H^\pm \rightarrow h^0 W^\pm$	23
3.5.1	Signal and Background	23
3.5.2	Analysis	27
3.5.3	Results 1	29
3.5.4	Results 2	30
3.6	The process $H^\pm \rightarrow t\bar{b}/\bar{t}b$	35
4	Discussion and future prospects	36
	References	39

1 Introduction

This chapter covers the basic background of Higgs physics and Supersymmetry in particle physics. The reader is assumed to be familiar with Quantum Field Theory, such as the first part in [1], elementary particle physics phenomenology such as [2] and the Gauge-principle. The first sections covers the Higgs boson in the Standard Model of elementary particle physics (SM) and why SM needs to be extended. The later sections motivates and introduces supersymmetry and Higgs physics in some supersymmetric models.

1.1 The Higgs boson in the Standard Model

The fermions of the Electroweak Standard Model (EWSM) are arranged according to:¹

$$\begin{bmatrix} \nu_\ell & \mathcal{U} \\ \ell^- & \mathcal{D}' \end{bmatrix},$$

which is called a generation, where:

$$\ell = e, \mu, \tau. \quad \mathcal{U} = u, c, t. \quad \mathcal{D}' = d', s', b'.$$

We thus have three generation of elementary particles. The primes on the quarks represents the fact that the quark eigenstates of the weak interactions are not the same as the (strong) mass eigenstates, but they are related by an unitary 3×3 matrix. The fermions can be divided into:

$$\begin{pmatrix} \nu_\ell \\ \ell \end{pmatrix}_L, \quad \begin{pmatrix} \mathcal{U} \\ \mathcal{D}' \end{pmatrix}_L, \quad \ell_R^-, \quad u_R, \quad d_{R'}.$$

The left-handed fermions are $SU(2)_L$ - doublets, and the right-handed fermions are $SU(2)_L$ - singlets. This is due to the observation that only left-handed fermions and right-handed anti-fermions participate in the weak interactions. Take note that there are no right-handed neutrinos in this scheme. One can show that no mass terms for the fermions are allowed in a Lagrangian due to the $SU(2)_L$ symmetry. The term $m_f^2 \bar{\psi}\psi = m_f^2 (\bar{\psi}_R \psi_L + \bar{\psi}_L \psi_R)$ is not invariant under this symmetry, so in the standard model, the fermions should be massless, contrary to experiment. The gauge-field quanta of EWSM, the γ , W^\pm and the Z^0 , can not have a mass term in the Lagrangian either, both due to $SU(2)_L$ invariance and renormalizability. In the case of the photon, this is satisfied, but the W^\pm , Z^0 are approximately 100 times heavier than the proton.

Fortunately, this problem is solved, the solution is called the Higgs Mechanism, which is a form of spontaneous symmetry breaking. In the EWSM we add a $SU(2)_L$ - doublet complex scalar field,

$$\phi = \begin{pmatrix} \phi^+ \\ \phi^0 \end{pmatrix},$$

¹The details of this section can be found in the literature e.g. [9]

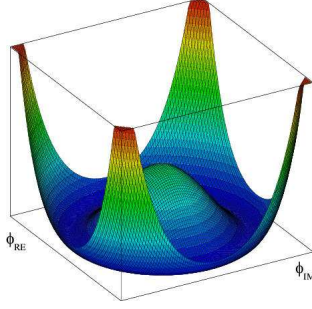


Figure 1: *The Mexican Hat shaped Higgs potential in the Standard Model.*

to the Lagrangian, with potential energy term: $V(\phi) = \mu^2\phi^\dagger\phi - h(\phi^\dagger\phi)^2$, which has the shape according to figure 1, for $\mu^2 < 0$.

The potential has an infinite number of states with minimum energy: $|\langle\phi^0\rangle| = \sqrt{-\mu^2/2h} \equiv v/\sqrt{2}$. The scalar doublet can be parametrized as:

$$\phi(x) = \exp\left(i\frac{\sigma_i}{2}\theta_i(x)\right) \frac{1}{\sqrt{2}} \begin{pmatrix} 0 \\ v - H(x) \end{pmatrix},$$

where we have four real fields; $\theta_i(x)$ and $H(x)$. Using that the Lagrangian is $SU(2)_L$ -invariant, we can choose $\theta_i(x) = 0$, this is the effect of choosing one particular ground state within the valley of the Mexican Hat potential, i.e. the symmetry is broken.

The covariant derivative of this scalar field is:

$$D_\mu\phi = \left(\partial_\mu + ig\frac{\sigma_i}{2}W_{i\mu} + ig'\frac{1}{2}B_\mu\right)\phi.$$

The W, B fields are the EWSM $SU(2)_L \otimes U(1)_Y$ fields. The charged W -bosons of the SM are linear combinations of the 1st and 2nd component of the W -field. The photon and the Z -boson of SM are linear combinations of the 3rd W -component and the B -field, expressed in terms of a rotation angle θ_W , called the Weinberg angle. The Electroweak unification condition occurs when $g \sin \theta_W = g' \cos \theta_W = Q_e$.

This symmetry breaking in the kinetic term of the Lagrangian results in mass terms for the W - and the Z -bosons:

$$(D_\mu\phi)^\dagger D^\mu\phi \rightarrow \frac{1}{2}\partial_\mu H\partial^\mu H + (v - H)^2 \left(\frac{g^2}{4}W_\mu^\dagger W^\mu - \frac{g'^2}{8\cos^2\theta_W}Z_\mu Z^\mu \right).$$

The masses of the W - and the Z -bosons are related by: $M_Z \cos \theta_W = M_W = \frac{1}{2}vg$. If we compute the entire Lagrangian we will also generate a new physical particle, the Higgs boson, with mass: $M_H = \sqrt{2}hv = \sqrt{-2\mu^2}$. Now one can also include masses for the fermions by introducing Yukawa couplings between them and the Higgs field. The strength of the coupling is proportional to the fermion mass. From the Fermi coupling constant, G_F , and the ratio of the W -mass and the Z -mass we obtain values for the Weinberg angles which agree. The vacuum expectation value (v) is obtained from G_F , (v) = 174 GeV. What is left to determine is the mass (and the existence) of the Higgs boson, which is a parameter in the Higgs Mechanism. All experimental searches for the Higgs boson have failed so far. Direct

searches by LEP and the Tevatron have drawn the conclusion that it should have a mass above 114 GeV and not between 160-170 GeV. One of the major scientific goals of the LHC is to find and determine the mass of the Higgs boson.

1.2 Why extend the Standard Model?

The Standard model of elementary particles with its $U(1)_Y \otimes SU(2)_L \otimes SU(3)_C$ symmetry has been very satisfactory experimentally. From it we have deduced the running coupling constants of the electromagnetic and the color force, the mass ratios of the W and Z boson, the existence of gluon jets, cross sections, mixing of weak and color eigenstates among quarks and several other experimental findings and several Nobel Prizes. But it has many shortcomings, some of them are to be mentioned now and after that we will argue why SUSY might be a good candidate for extending the SM.

- **Quantum Gravity** The standard model only describes three of the four known forces, the missing piece is gravity. Constructing a Quantum Field Theory of gravity has not been quite successful though. The gravitational field is described by rank-2 tensors in Einstein's General Theory of Gravity, the field-quanta, called the *graviton*, is hence a spin-2 particle [1]. Since gravity is an infinite range force, just as electromagnetism, the graviton should be massless. However, due to the Weinberg-Witten Theorem, a quantum field theory with massless field quanta which spin is greater than 1 can not simultaneously be Lorentz Invariant and Renormalizable [3].
- **Unification of Forces** The unification of physical phenomena into one bigger, more general, scheme, has been a goal in physics since the days of J. Maxwell when he unified the electric force with magnetism into electromagnetism. The success of unifying the electromagnetic force with the weak force, made one optimistic in unifying the color force with the electroweak. A necessary condition for this to occur is that the couplings should meet at the same point at a given energy. The standard textbook example of such a Grand Unified Theory (GUT) is $SU(5)$, which will be broken into the SM $U(1) \otimes SU(2) \otimes SU(3)$. The condition for this to occur is:

$$g_5 = g_3 = g = \sqrt{\frac{5}{3}} g',$$

where g_5 is the $SU(5)$ gauge unification condition, g_3 is the $SU(3)_C$ gauge coupling, g is the $SU(2)$ -electroweak coupling and g' the $U(1)$ -coupling [1]. Since we know the renormalization group equations for g , g' and g_3 we can extrapolate and find out that they don't meet at one unification point, they miss each other and form a triangle around $10^{13} - 10^{15}$ GeV, see figure 2.

- **The hierarchy problem** The physical parameter which sets the scale for all masses in the electroweak theory is the vacuum expectation value (vev) of the Higgs field, $v = \sqrt{\mu^2/\hbar} = 174$ GeV. The one loop correction to μ^2 is quadratic in the cut-off: Λ^2 , and since the electroweak theory is renormalizable, we can let Λ go to infinity.

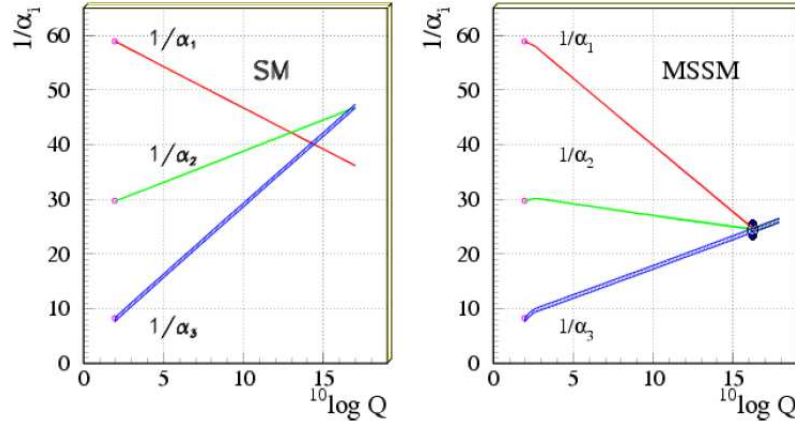


Figure 2: *The running of the gauge couplings for electromagnetism, the weak- and the strong force in the SM and in the MSSM [4].*

Thus the theory is well-defined and one can calculate anything up to, in practice, infinite energies [5]. But as implied earlier, we would like to include gravity, and the scale where gravity, i.e. new physics, becomes important is the Planck mass-scale: $m_{\text{Planck}} \sim 10^{19}\text{GeV}$. Now this is what is called 'fine tuning' - in that sense that the Lagrangian parameter μ^2 goes from $\sim (10^{19}\text{GeV})^2$ to $\sim (10^2\text{GeV})^2$.

- **Dark Matter** The ordinary matter, called *baryonic*² only constitute about 4% of the total energy density of the universe (Ω). One has found that about 70% is made up of something called *dark energy* - which has the effect of a repulsive gravitation. The rest of the energy density content is called *dark matter*. The dark matter does not interact with the electromagnetic force, and has been found by studying e.g. velocity distributions in galaxies and gravitational lensing of galaxy clusters. The only particle in the Standard Model which can contribute to this is the neutrino. The density contribution to the dark matter of relic neutrinos is only of the order 1% [6].

1.3 Supersymmetry in Particle Physics

This section covers the very basics of supersymmetry and how it affects the particle spectra. Detailed introduction to supersymmetry can be found in e.g. [5, 8].

1.3.1 The Supersymmetry

There are two kinds of symmetries in physics, space-time symmetry and internal symmetry. The space-time symmetries are translations and Lorentz transformations which together constitute the Poincaré symmetry. An example of internal symmetry is the $SU(3)$ colour symmetry in QCD - the theory of quarks and gluons. The generators for the Poincaré symmetry commute trivially with all internal symmetry generators. It can be shown that

²i.e. atomic nuclei and electrons

the only way to extend the Poincaré symmetry to allow non-trivial commutators with the internal symmetry generators is to include transformations between bosonic and fermionic degrees of freedom. In other words, we consider fermionic space-time generators Q^α which act, schematically, according to:

$$Q^\alpha |\text{boson}\rangle = |\text{fermion}\rangle^\alpha$$

$$Q^\alpha |\text{fermion}\rangle_\alpha = |\text{boson}\rangle$$

The inclusion of the fermionic generators Q^α is the basis of supersymmetry.

Now, since the SUSY generators trivially commute with the internal symmetry generators, the fields will have the same internal quantum numbers. In the case of the Standard Model, the superpartners will have the same isospin, color and electric charge, e.g.:

$$\text{Right handed electron } e_R \leftrightarrow \tilde{e}_R \text{ selectron ,}$$

the $\tilde{}$ denotes SUSY partner (superpartner), and the R on the selectron is superfluous since a spin-0 particle has no chirality but is there only to show that it belongs to the $SU(2)_L$ singlet *supermultiplet*. Since the SUSY generators are fermionic, supermultiplets will consist of particles that differs with spin $\frac{1}{2}$, thus we will have vector supermultiplets with a massless vector field with spin-1 with a spin- $\frac{1}{2}$ superpartner, e.g.:

$$\text{gluon } g_a \leftrightarrow \tilde{g}_a \text{ gluino .}$$

In the case of the complex scalar doublet field ϕ , as we had in section 1.1, one can not have terms of the kind $\phi^\dagger \phi$ consistent with supersymmetry. Thus, we need two independent scalar doublets:

$$H_1 : \begin{pmatrix} H_1^0 \\ H_1^- \end{pmatrix}, \quad H_2 : \begin{pmatrix} H_2^+ \\ H_2^0 \end{pmatrix},$$

with corresponding spin 1/2 fields.

The basic building blocks for a supersymmetric Lagrangian are the superfields ϕ and the superpotential W . A superfield is a field defined over the superspace: space-time and fermionic degrees of freedom and the superpotential is a function of superfields. Including the gauge symmetries, thus we consider a Lagrangian with a combination of super- and gauge symmetries, one obtain the following generic scalar potential:

$$V(\phi_i, \phi_i^\dagger) = |W_i|^2 + \frac{1}{2} \sum_G \sum_\alpha \sum_{i,j} g_G^2 \left(\phi_i^\dagger T_G^\alpha \phi_i \right) \left(\phi_j^\dagger T_G^\alpha \phi_j \right), \quad (1)$$

where G is a gauge group label (i.e. $SU(2)$, $SU(3)$, $U(1)$) and g_G, T_G is the gauge coupling and the generator of that gauge group respectively. The term W_i is the partial derivative of the superpotential with respect to the superfield ϕ_i :

$$W_i = \frac{\partial W}{\partial \phi_i} = M_{ij} + \frac{1}{2} y_{ijk} \phi_j \phi_k,$$

where M_{ij} is the mass matrix for the fermions and y_{ijk} are Yukawa couplings.

Since the SUSY generators commute with the Poincaré generators, especially the four-momentum operator P^μ , the SM particles and their superpartners should have the same rest masses. But this is not found. Thus supersymmetry is a broken symmetry in nature, and one must include SUSY-breaking terms in the Lagrangian. One can do this is by considering a parametrization for the SUSY-breaking, valid at “low” energies. One requires that these new terms should have positive mass-dimension, i.e. “Soft”, so that no new divergences appear in the theory. One example of a Soft SUSY-breaking term is the mass-squared term for the sleptons:

$$-m_{\tilde{L}_{ij}}^2 \tilde{L}_i^\dagger \cdot \tilde{L}_j - m_{\tilde{e}_{ij}}^2 \tilde{e}_{L_i}^\dagger \tilde{e}_{L_j}, \quad (2)$$

where the dot product is $SU(2)_L$ invariant, e.g. for the Higgs-fields:

$$H_2 \cdot H_1 = H_2(-i\sigma_2)H_1 = H_2^+ H_1^- - H_2^0 H_1^0,$$

where σ_2 is the second pauli matrix. The Soft SUSY-breaking terms are responsible for the large number of free parameters in the SUSY-models in particle physics, in the Minimal Supersymmetric Standard Model (MSSM) there are over 100 free parameters.

More implications of supersymmetry to particle physics are outlined in section 1.4.

1.3.2 Supersymmetric Higgs bosons

MSSM The theory with minimal inclusion of terms which is SUSY-invariant and gauge-invariant is called the *Minimal Supersymmetric Standard Model* (MSSM). The particle content is as in the Standard Model plus the previous mentioned 2-Higgs doublet fields and superpartners to each of these.³ The Higgs-part of the superpotential for the MSSM is:

$$W_{\text{MSSM}}^{\text{Higgs}} = \mu H_1 \cdot H_2. \quad (3)$$

The other terms in the MSSM-superpotential are quark- and lepton-superfields coupled to the Higgs-superfields with the same Yukawa couplings as in the SM. Thus the only new parameter at this stage is the μ , which is not the same μ as in the SM Higgs potential. The term which will be included in the Lagrangian, the first term of eq. (1) is:

$$|\mu|^2 (|H_1^-|^2 + |H_1^0|^2 + |H_2^+|^2 + |H_2^0|^2). \quad (4)$$

The terms from the soft SUSY-breaking terms are:

$$m_1^2 (|H_1^-|^2 + |H_1^0|^2) + m_2^2 (|H_2^+|^2 + |H_2^0|^2) + \{ \mu_3^2 (H_1^- H_2^+ - H_1^0 H_2^0) + \text{h.c.} \}. \quad (5)$$

Including terms for the gauge couplings, $SU(2) : g, U(1) : g'/2$, the scalar potential in the MSSM is:

$$\begin{aligned} V = & \mu_1^2 (|H_1^-|^2 + |H_1^0|^2) + \mu_2^2 (|H_2^+|^2 + |H_2^0|^2) + \\ & \{ \mu_3^2 (H_1^- H_2^+ - H_1^0 H_2^0) + \text{h.c.} \} + \frac{g^2 + g'^2}{8} \{ |H_2^+|^2 + |H_2^0|^2 - |H_1^0|^2 - |H_1^-|^2 \}^2 + \\ & \frac{g^2}{2} |H_2^0 H_1^{-\dagger} - H_2^+ H_1^{0\dagger}|^2, \end{aligned} \quad (6)$$

³For a complete table, see e.g. [5] tables 8.1 and 8.3

where $\mu_1^2 \equiv |\mu|^2 + m_1^2$ and $\mu_2^2 \equiv |\mu|^2 + m_2^2$. In order to break the $SU(2)_L \otimes U(1)_Y$ symmetry, the potential should have a non-zero minimum for the neutral Higgs fields. We can choose both $H_2^+ = 0$ and $H_1^- = 0$, thus electromagnetism remains unbroken. Now, for the neutral fields, the potential becomes:

$$V_n = \mu_1^2 |H_1^0|^2 + \mu_1^2 |H_2^0|^2 - 2\mu_3^2 |H_1^0| |H_2^0| + \frac{g^2 + g'^2}{8} (|H_1^0|^2 - |H_2^0|^2)^2. \quad (7)$$

The potential depends on three parameters, the μ_i^2 's. It is bounded from below if:

$$\mu_1^2 + \mu_2^2 > 2\mu_3^2 > 0,$$

and the origin is not the minimum if:

$$\mu_1^2 \mu_2^2 < \mu_3^4.$$

The Higgs mechanism, i.e. when H_1^0 and H_2^0 acquire non-zero vacuum expectation value, leads to the following relations [5]:

$$m_Z^2 = \frac{1}{2}(g^2 + g'^2)(v_1^2 + v_2^2),$$

$$m_W^2 = \frac{1}{2}g^2(v_1^2 + v_2^2),$$

$$(|\mu|^2 + m_1^2) = b \tan \beta - (m_Z^2/2) \cos 2\beta,$$

$$(|\mu|^2 + m_2^2) = b \cot \beta + (m_Z^2/2) \cos 2\beta,$$

with v_i the vacuum expectation value for H_i^0 , $v_1^2 + v_2^2 = 174$ GeV and $\tan \beta \equiv v_2/v_1$.

In the SM, we had four scalar degrees of freedom to start with, after the electroweak symmetry breaking, three of these became the longitudinal modes for the Z and W -bosons and the last one became the physical new scalar particle, the Higgs boson. In the MSSM we have eight scalar degrees of freedom, resulting in five Higgs bosons. The (tree-level) masses for these are found by expanding the quadratic terms of the Lagrangian around its minimum (the v_i -values), the results are:

$$m_{A^0}^2 = \frac{2\mu_3^2}{\sin 2\beta},$$

$$m_{H^\pm}^2 = m_W^2 + m_{A^0}^2,$$

$$m_{h^0, H^0}^2 = \frac{1}{2} \left[m_Z^2 + m_{A^0}^2 \mp \sqrt{(m_Z^2 + m_{A^0}^2)^2 - 4m_{A^0}^2 m_Z^2 \cos^2 2\beta} \right].$$

The h^0 is the lightest Higgs boson and is the corresponding SM-Higgs. At tree-level, its mass is constrained by:

$$m_{h^0} \leq m_Z |\cos 2\beta| \leq m_Z.$$

Inclusion of loop contribution from top quarks and stop squarks will increase this limit.

NMSSM A problem with the MSSM is the so called μ -problem.⁴ An attempt to solve this is to include yet another Higgs field, a singlet S . This model is called NMSSM, which means *Next to* - MSSM, and its superpotential is the same as for the MSSM except for the Higgs-part, which is replaced by:

$$W_{\text{NMSSM}}^{\text{Higgs}} = \lambda S H_1 \cdot H_2 + \frac{\kappa}{3} S^3, \quad (8)$$

where $\lambda(S) = \mu$ in the superpotential for the MSSM, eq. (4). The soft SUSY-breaking terms will be a little bit more involved than in the MSSM case but follow the same scheme. The extra singlet will give two additional neutral Higgs states which will mix with the previous neutral states to produce quite complicated mass-formula for the neutral Higgs bosons [11]. However, the charged Higgs bosons will have the simple mass relation $m_{H^\pm}^2 = m_W^2 + m_{A^0}^2 - \lambda^2(v_1^2 + v_2^2)$, where the $m_{A^0}^2$ is not defined in the same way as in the MSSM. Another feature of the NMSSM is that the mass of the lightest Higgs does not have the constraint as in the MSSM, where large stop-loop contributions are required to have m_h above the current experimental lower limit. These contributions will affect the Z -boson mass which will receive a *fine tuning* which many theoreticians dislike.

The SUSY model which this thesis treats is an Effective Field Theory - simplification of the NMSSM, see chapter 2.

1.4 Why Supersymmetry?

- **New particles and forces** Supersymmetry is a symmetry between bosons and fermions, the transformation of a bosonic field will yield a fermionic field - and vice versa. Each fermion in the standard model will have bosonic *superpartner* and vice versa, for instance we can have:

electron \leftrightarrow selectron

W-boson \leftrightarrow wino.

One consequence of these new particles is that we now can have candidates for Dark Matter; if some of these superpartner particles are stable they can still be around and contribute to the energy-density of the universe [7].

Another feature is that it can remove the fine tuning of the Higgs mass renormalization. The reason for this is that loop corrections to fermion masses goes as $\delta m \sim m \ln \Lambda$, thus, even for $\Lambda \sim \mathcal{O}(10^{19})\text{GeV}$, we still have $\delta m \sim m$. So now we have the starting point to remove this fine tuning - the fermionic superpartner loops will exactly cancel the quadratic divergence of the Higgs mass[5].

- **A new kind of symmetry** The gauge symmetries and other internal symmetries trivially commute with the Poincaré group generators⁵. The so far only known non-trivial extension to the Poincaré group is the Supersymmetric algebra which thus introduces a new symmetry in space-time.

⁴See e.g. [5] page 125.

⁵the group of boosts, rotations and translations in space-time

- **Gauge coupling unification** Including the contribution from supersymmetric particles in the loop diagrams, one finds that unification of the three gauge couplings are possible, see figure 2.
- **Supergravity** Another appealing feature of supersymmetry is that gravity will emerge when considering *local* SUSY transformations [7].

1.5 Outline

The task for this thesis was to examine the Higgs sector of the so called λ SUSY model, in particular the phenomenology of the charged Higgs bosons. The thesis also treats a benchmark study of the detection possibility of the charged Higgs bosons at the CERN LHC. The outline for the rest of this thesis is organized as follows: We first give an introduction to the λ SUSY model and its Higgs sector within the two-Higgs-doublet model. After that we present the Monte Carlo tools used for the benchmark point studies and the results. Finally we end the thesis with a discussion of the obtained results and give some future prospects.

2 The λ SUSY model

2.1 Motivation

At this stage no signal of supersymmetry or Higgs bosons has been found in experiments. Motivated by this, the authors of [12] have considered a special version of NMSSM, where the masses of the Higgs bosons become larger than in e.g. MSSM. The field content is the same as in the NMSSM but one takes the coupling λ to be “large” at the EW energy scale. Since λ is a parameter in the Lagrangian, it will due to renormalization be energy-dependent. This property is given by its renormalization group equation:

$$\frac{d\lambda^2}{d\ln E} = \frac{\lambda^4}{2\pi^2}.$$

In [12] λ is taken to be $\lambda(500 \text{ GeV}) \approx 2$. Thus the theory is only perturbative up to about 10 TeV and is to be considered an Effective Field Theory. At energy scales above 10 TeV, new physics should appear, e.g. compositeness of the Higgs bosons. The general form of the Higgs superpotential is:

$$W = \mu(S) H_1 H_2 + f(S), \quad (9)$$

where μ and f are functions of the singlet superfield S . Since λ will be large, one can as a simplification neglect the gauge terms, this yields the following scalar potential:

$$\mathbb{V} = \mu_1^2(S) H_1 \cdot H_1^\dagger + \mu_2^2(S) H_2 \cdot H_2^\dagger - (\mu_3^2(S) H_1 \cdot H_2 + \text{h.c.}) + \lambda^2 |H_1 \cdot H_2|^2 + V(S), \quad (10)$$

Where $\lambda = \partial\mu/\partial S$. The functions $\mu_i(S)$ will after electroweak symmetry breaking be evaluated at $S = \langle S \rangle \equiv s$, and we will call $\mu_i \equiv \mu_i(s)$. Following [12] W and \mathbb{V} are assumed to be \mathcal{CP} -invariant. The scalar potential is stable for $\mu_1^2, \mu_2^2 > |\mu|^2$ and we can have electroweak symmetry breaking if $|\mu_3^2| > \mu_1\mu_2$ is satisfied at the minimum of the potential.

2.2 Higgs Sector

2.2.1 Mass Relations

The relations one obtains by minimizing the potential are:

$$\tan \beta = \frac{\mu_1}{\mu_2}, \quad (11)$$

$$\lambda^2 v^2 + \mu_1^2 + \mu_2^2 = \frac{2\mu_3^2}{\sin 2\beta}, \quad (12)$$

where $v^2 \equiv v_1^2 + v_2^2 = (174 \text{ GeV})^2$. The tree level mass for the charged higgs is:

$$m_{H^\pm}^2 = \mu_1^2 + \mu_2^2 = 2\mu_3^2 / \sin 2\beta - \lambda^2 v^2. \quad (13)$$

In [12] one takes the mass of the singlet scalar S to be much larger than the other higgs bosons, and one neglects mixing with the other neutral scalars in the theory. Thus the relation for tree level masses becomes quite simple. The pseudoscalar Higgs A^0 :

$$m_{A^0}^2 = 2\mu_3^2 / \sin 2\beta = m_{H^\pm}^2 + \lambda^2 v^2. \quad (14)$$

The \mathcal{CP} -even states $h_i = \sqrt{2}(\text{Re } H_1^0)$ have the following mass-matrix:

$$\begin{pmatrix} m_{A^0}^2 \sin^2 \beta & (\lambda^2 v^2 - m_{A^0}^2/2) \sin 2\beta \\ (\lambda^2 v^2 - m_{A^0}^2/2) \sin 2\beta & m_{A^0}^2 \cos^2 \beta \end{pmatrix}, \quad (15)$$

and have the following eigenvalues and eigenstates:

$$m_{h^0, H^0}^2 = \frac{1}{2} (m_{A^0}^2 \pm X), \quad (16)$$

$$X^2 = m_{A^0}^4 - 4\lambda^2 v^2 m_{H^\pm}^2 \sin^2 2\beta, \quad (17)$$

$$H^0 = \cos \alpha h_1 + \sin \alpha h_2, \quad h^0 = \sin \alpha h_1 + \cos \alpha h_2, \quad (18)$$

$$\alpha = \arctan \left\{ \frac{m_{A^0}^2 \cos 2\beta + X}{(\lambda^2 v^2 - m_{H^\pm}^2) \sin 2\beta} \right\}. \quad (19)$$

One also has the following inequalities [12, 13]:

$$m_{h^0} \leq \lambda v \sin \beta,$$

$$m_{h^0} < m_{H^\pm} < m_{H^0} < m_{A^0},$$

the fixed ordering for the mass spectrum is a peculiarity of λ SUSY. The Higgs sector can be parametrized by the charged Higgs mass, m_{H^\pm} , $\tan \beta$ and λ . The mass spectrum as a function of these parameters is shown in figure 3. The inclusion of the gauge-terms in the potential eq. (10) will e.g. increase the m_{h^0} with 5-10 GeV and the mixing effect of the singlet S is approximate 5-10% [13].

2.2.2 Phenomenology of the λ SUSY Higgs sector within the 2HDM.

Since the singlet S decouples in this approximation, the Higgs sector of λ SUSY is a two-Higgs doublet and its properties can be expressed by considering the two-Higgs doublet model (2HDM). The 2HDM potential is the most general gauge invariant and renormalizable potential that one can form with two Higgs doublets:

$$\begin{aligned} \mathbb{V}_{2\text{HDM}} = & m_{11}^2 \phi_1^\dagger \phi_1 + m_{22}^2 \phi_2^\dagger \phi_2 - \left[m_{12}^2 \phi_1^\dagger \phi_2 + \text{h.c.} \right] \\ & + \frac{1}{2} \lambda_1 (\phi_1^\dagger \phi_1)^2 + \frac{1}{2} \lambda_2 (\phi_2^\dagger \phi_2)^2 + \lambda_3 (\phi_1^\dagger \phi_1) (\phi_2^\dagger \phi_2) + \lambda_4 (\phi_1^\dagger \phi_2) (\phi_2^\dagger \phi_1) \quad (20) \\ & + \left\{ \frac{1}{2} \lambda_5 (\phi_1^\dagger \phi_2)^2 + \left[\lambda_6 (\phi_1^\dagger \phi_1) + \lambda_7 (\phi_2^\dagger \phi_2) \right] (\phi_1^\dagger \phi_2) + \text{h.c.} \right\}. \end{aligned}$$

To determine the most relevant decay modes and their Branching Ratio, we use the Two-Higgs-Doublet Model Calculator (2HDMC), a C++ program developed by the Uppsala theory group [14]. In the 2HDMC, \mathcal{CP} -violation is not yet implemented. The user writes his/her own main program which uses an instance of a class representing the underlying 2HDM. The model is set by giving the values of the parameters λ_i , $\tan \beta$, $\sin(\beta - \alpha)$ and the Yukawa couplings. To specify the Higgs masses, we can either fix the m_{ij} values, or simply put them by hand. After one has set the model, one can deduce total- and partial decay widths for the Higgses by using the corresponding member functions.

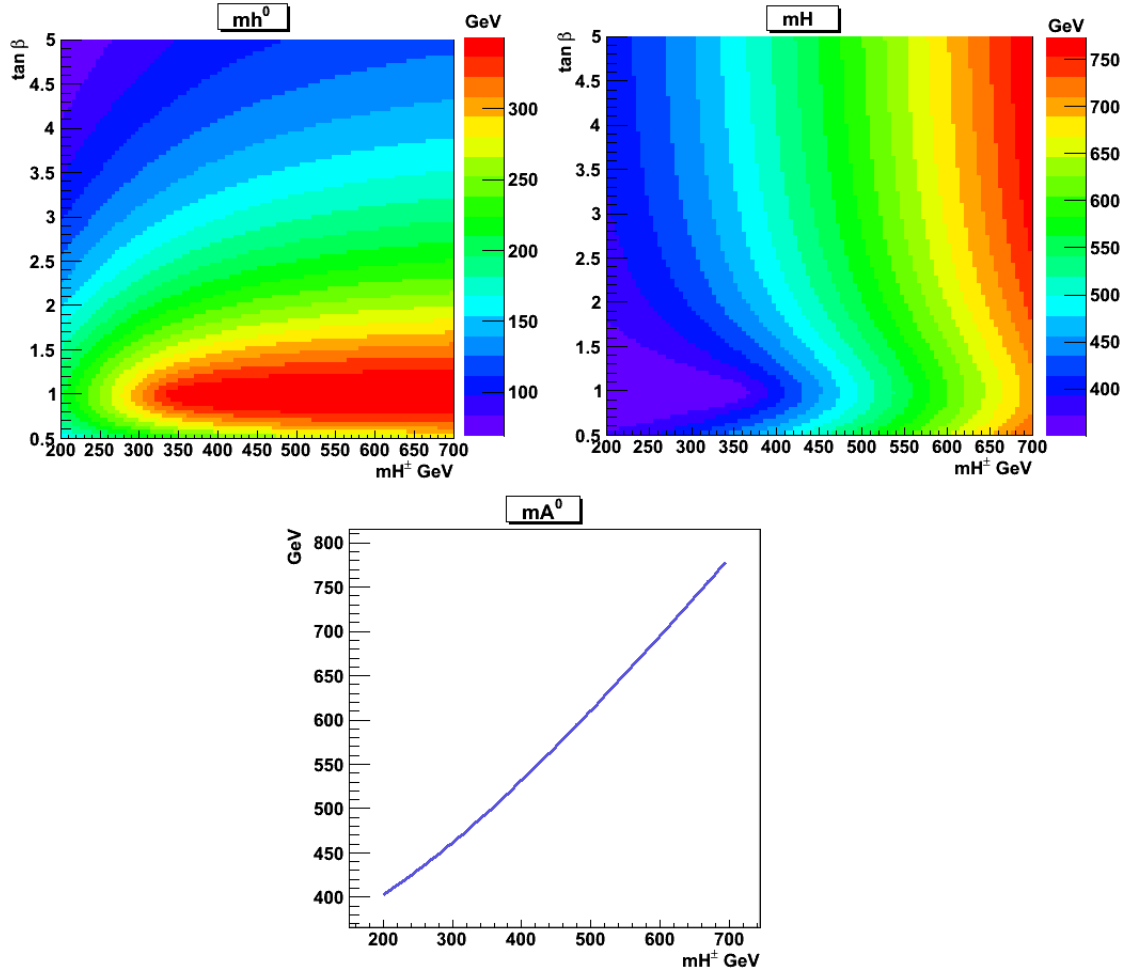
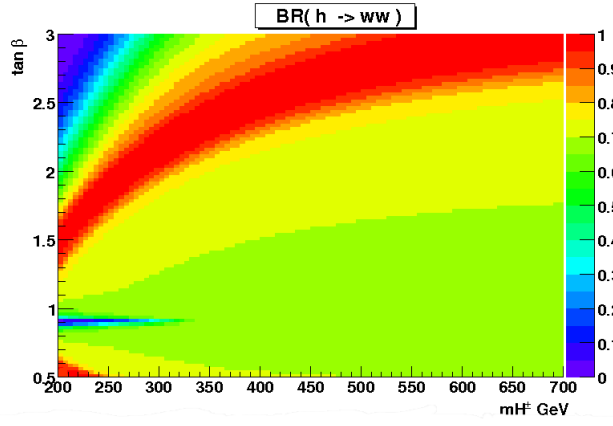


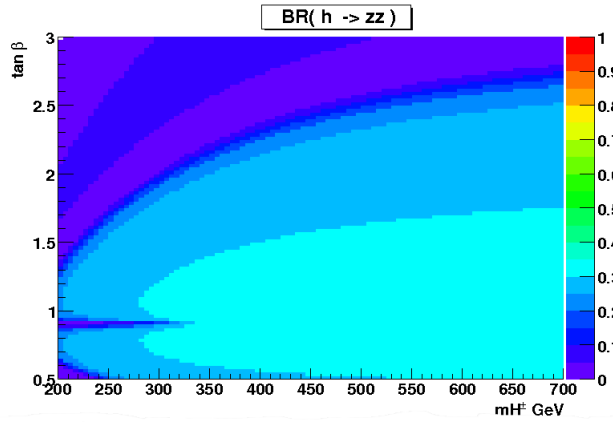
Figure 3: The neutral Higgs masses in λ SUSY as a function of m_{H^\pm} and $\tan \beta$. The value of λ is taken to be equal to 2.0.

We obtain the λ SUSY potential eq. (10) by using the member function `set_param_phys`, where the user specifies the 2HDM by giving the physical Higgs masses, $\sin(\beta - \alpha)$, λ_6 , λ_7 , m_{12}^2 and $\tan \beta$. In our case we have m_{H^\pm} and $\tan \beta$ as parameters and thus give the neutral Higgs masses, $\sin(\beta - \alpha)$ and $m_{12}^2 = \mu_3^2$ in terms of these parameters using equations (13), (14), (16) and (19). The λ_6 and λ_7 are put to zero. Figures 4, 5, 6 and 7 are produced by evaluating the input parameters for each point on a grid over $(m_{H^\pm}, \tan \beta)$ space, passing these over to the model and then fill the corresponding bin in a ROOT⁶ 2D-histogram with the evaluated Branching Ratios. As can be seen in figure 3, a large h^0 mass is obtained for quite small $\tan \beta$; $\tan \beta \lesssim 3.0$.

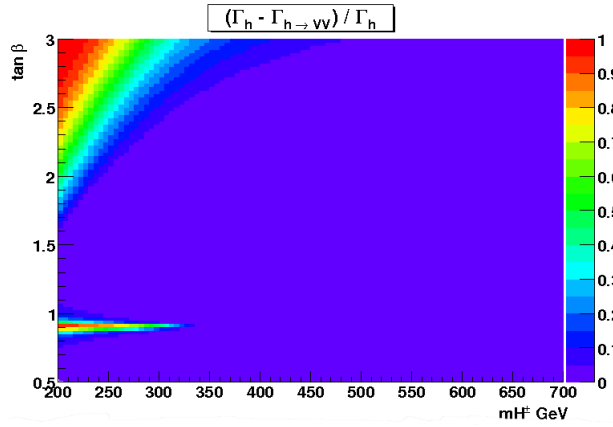
⁶ROOT is a C++ analysis package for physics and graphics developed by CERN, <http://root.cern.ch>



(a) $h^0 \rightarrow W^\pm W^\mp$

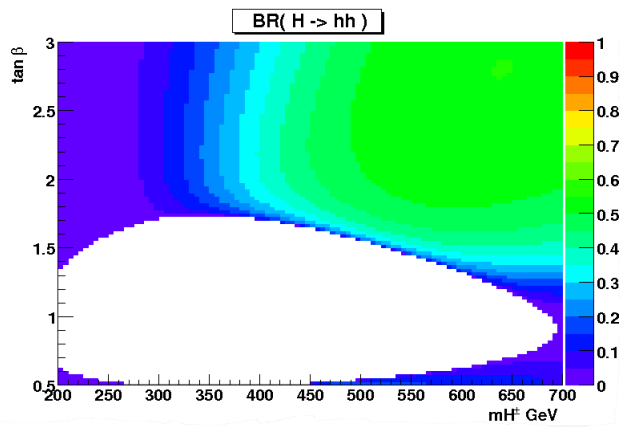


(b) $h^0 \rightarrow Z^0 Z^0$

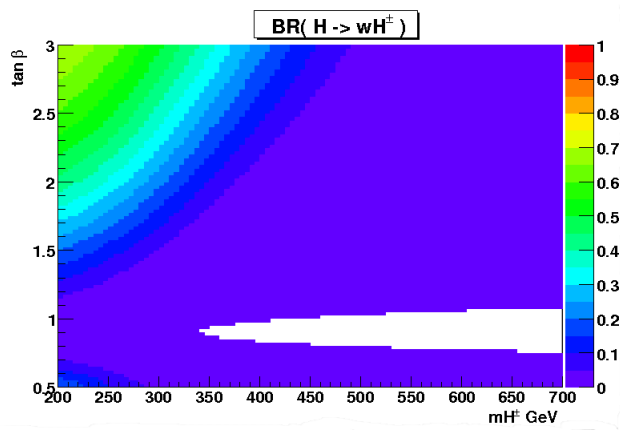


(c) $h^0 \rightarrow b\bar{b}/\gamma\gamma/c\bar{c}/\dots$

Figure 4: Branching Ratios for the h^0 in the λ SUSY model as functions of m_{H^\pm} and $\tan\beta$ using the 2HDMC.

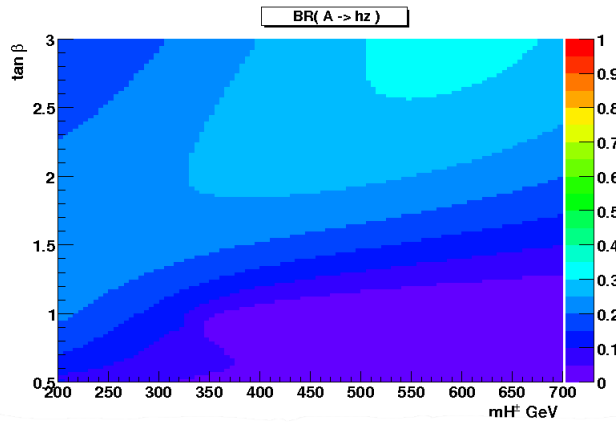


(a) $H^0 \rightarrow h^0 h^0$

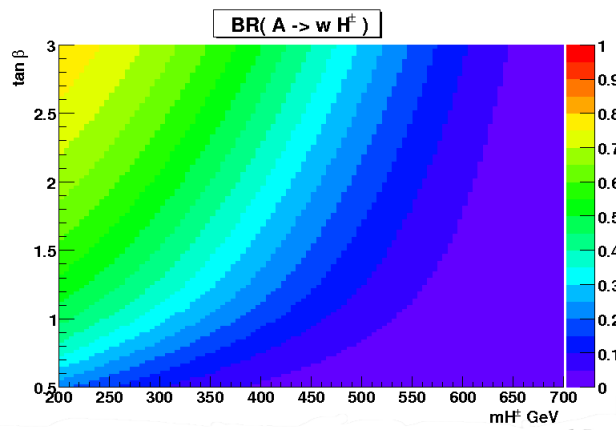


(b) $H^0 \rightarrow H^\pm W^\mp$

Figure 5: Branching Ratios for the H^0 in the λ SUSY model.

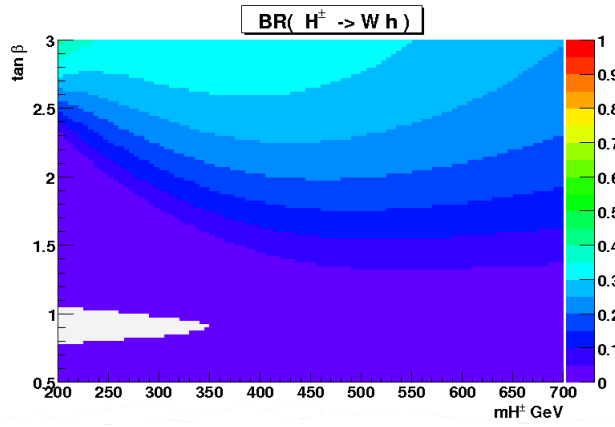


(a) $A^0 \rightarrow h^0 Z^0$

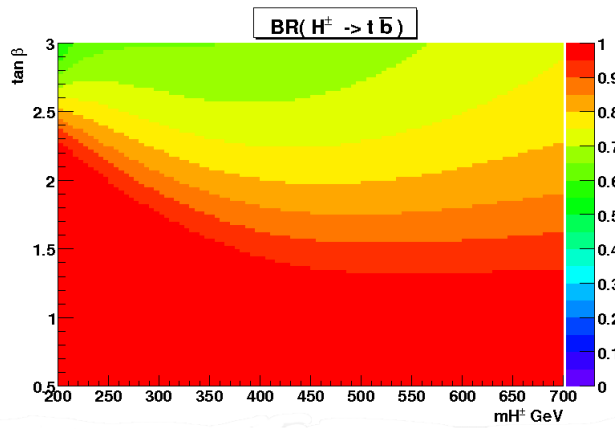


(b) $A^0 \rightarrow H^\pm W^\mp$

Figure 6: Branching Ratios for the A^0 in the λ SUSY model.



(a) $H^\pm \rightarrow h^0 W^\pm$



(b) $H^\pm \rightarrow t\bar{b}/\bar{t}b$

Figure 7: Branching Ratios for the H^\pm in the λ SUSY model.

3 Benchmark point studies

In this chapter, we examine if charged Higgs bosons in λ SUSY can be seen at the CERN LHC. The article [13] deals with the H^0 and A^0 bosons using a simplified partonic analysis. Here, we will perform a complete analysis with parton showering, hadronization and jet-finding.

3.1 Event Generation

The LHC at CERN will collide protons to produce new particles but it is not the protons which are the particles undergoing the so called *hard* scattering event. Instead, it is their substructure particles, i.e. their quark- and gluon-content which is responsible for this. These substructure-particles are often called *partons* and how the different partons build up the proton are described by the parton distribution functions (PDF's) which are Q^2 - four-momentum transfer - dependent. This Q^2 dependence of the PDF's means that depending on the energy at which we are colliding our protons, the most part of the actual hard interactions might be due to gluon-gluon scattering, or up-antiup etc. We must weight the cross section of a particular process with the PDF's to obtain the correct result. So, if we want to study process $gg \rightarrow t\bar{t}$ at pp collisions, we have several hundred of incoming particles which may collide, radiate and interfere. But the story is not over, we want to know in which direction all of these particles will go, and with what energy. And since we do not have free quarks and gluons and nature, they will undergo a process called hadronization - they will form hadrons which there are a couple of models existing for describing this.

As the reader might have guessed, even to fully determine the properties of a *single* pp -event will become too cumbersome for anyone, evaluating several hundred of integrals and differential equations. Over the course of years (decades) one has developed so called *event generators*, where the user specifies what process he/she would like to study and a program will produce a record over all final state particles and their four-vectors etc. These programs uses the Monte Carlo method to evaluate e.g. the many-dimensional phase space integrals involved in the processes.

The programs used in this thesis are `Pythia 8.125` and `MadGraph/MadEvent` which will be described in the following sections.

3.2 Pythia Event Generator

`Pythia` was developed by the theory group at Lund, Sweden, in the early 1980's with the `Fortran` language. Due to the overall alignment towards `C++` in High Energy physics nowadays, one started to develop `Pythia` in `C++` language; `Pythia v.8`.

The structure of `Pythia` is roughly divided into three levels; **Process**-level, **Parton**-level and **Hadron**-level:

- **The Process level** is the hard interaction. `Pythia` comes with many possibilities to generate processes with one or two final state particles within the Standard Model and beyond, e.g. Higgs and SUSY. There is also an interface which allows the user to provide a complete hard event in terms of four-vectors from external generators, e.g. `MadGraph/MadEvent`, by files in the *Les Houches* format.
- **The Parton level** propagates the partons from the hard event in space-time and generate parton showering, multiple interactions, beam remnants etc.
- **The Hadron level** makes the hadronization, i.e. partons \rightarrow hadrons. `Pythia` implements the *Lund String Model*, where partons in a limited space-time region form strings in the colour-field between them. When the partons separates the potential energy between them can become so high that the string breaks, like a rubber band, and pulls out quarks-antiquarks from the vacuum, resulting in new parton-string entities. When the partons have lost energy in this process so that no further excitation of quarks and string breaking can occur, they will form hadrons. The Hadron level also forces particles to decay.

`Pythia 8` comes with some physics classes like four-vectors and histograms. Also there is a Jet-algorithm which is used in the present analyses. This Jet-algorithm is called `CellJet` and finds final state partons clustered around a high transverse energy *seed* parton within a certain radius in the (φ, η) plane⁷. The algorithm first finds the hardest ($E_T^{\max.}$) parton and then sums up all four-vectors for the partons within the user-specified radius: $\Delta R \equiv \sqrt{(\Delta\varphi)^2 + (\Delta\eta)^2}$. When this is done, the algorithm searches for the hardest parton outside this region and repeats the procedure of four-vector addition. The algorithm will continue until there is no seed-particle with energy above the minimum seed-energy given by the user. The user also specifies in which η -range and $\min. E_T^{\text{jet}}$ the algorithm should consider.

The user writes his/her own program which implements the `Pythia`-classes and methods, and one can modify masses, widths and decay-channels to a great extent by letting the main instance read strings in a certain `Pythia` format.

3.3 MadGraph/MadEvent

`MadGraph/MadEvent` are `Fortran`-programs which, given a process, evaluate the relevant Feynman diagrams at tree-level [17]. The program can also evaluate the matrix element modulus squared, total cross-section (over user defined phase-space regions) and generate (hard) events in *Les Houches*-format. The user provides `MadGraph/MadEvent` with the process one would like to study, how many events to generate and the desired phase-space region using input files called *cards*. There is also a possibility to run `MadGraph/MadEvent`

⁷ η is the *pseudorapidity*; $\eta = -\frac{1}{2} \ln(\tan(\frac{1}{2}\theta))$.

via a web interface on the homepage. The homepage also contains a library which contains samples for some of the most useful processes for LHC - physics.

3.4 Resonant Higgs production via Gluon fusion in pp -collisions

To produce the charged Higgs, we consider the production of A^0 in gluon-gluon fusion, see figure 8 a for Feynman diagram. The A^0 are then allowed to decay into $H^\pm W^\mp$, see figure 6(b) for Branching Ratio. `Pythia` can evaluate total cross sections, where the accuracy increases with the number of events generated. The total cross section for $gg \rightarrow A^0$ and its error are shown in figures 9 and 10. In figure 11 we have weighted the total production cross section with all the relevant branching ratios for some final states. We refer to the figure captions for further information. The A^0 can also be produced in $q\bar{q}$, where the \bar{q} must be a sea-antiquark from the proton. The cross section for this process is found to be much lower than in the gluon fusion, about two orders of magnitude for generic points in the $(m_{H^\pm}, \tan\beta)$ -space.

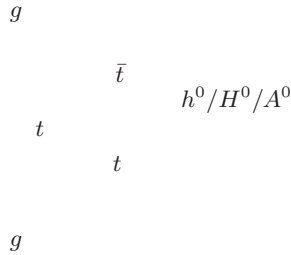


Figure 8: *One possible Feynmandiagram for gluon fusion Higgs production via a (top) quark loop.*

3.5 The process $H^\pm \rightarrow h^0 W^\pm$

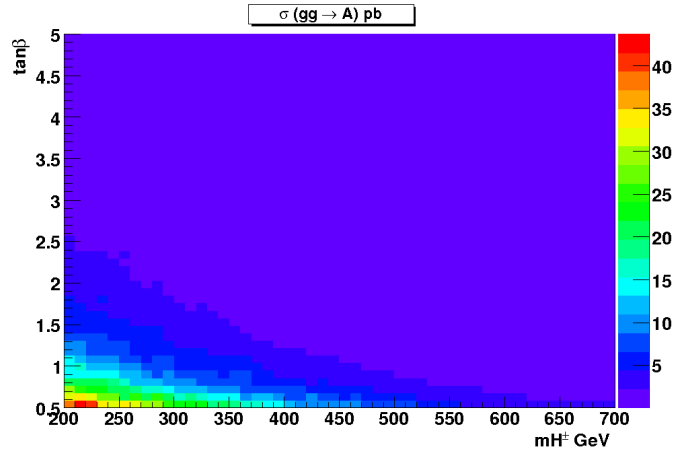
3.5.1 Signal and Background

Here we consider the cases where the A^0 -associated W decays leptonically and the W from H^\pm decays hadronically, and vice versa. These processes are treated separately. The h^0 decays into $2VV$, where $V \in [W, Z]$, which decays hadronically. To summarize, we have $h^0 \rightarrow 4j$ with $H^\pm \rightarrow 6j$ or $H^\pm \rightarrow \ell\nu 4j$, where $\ell = e, \mu$. As benchmark point, we choose:

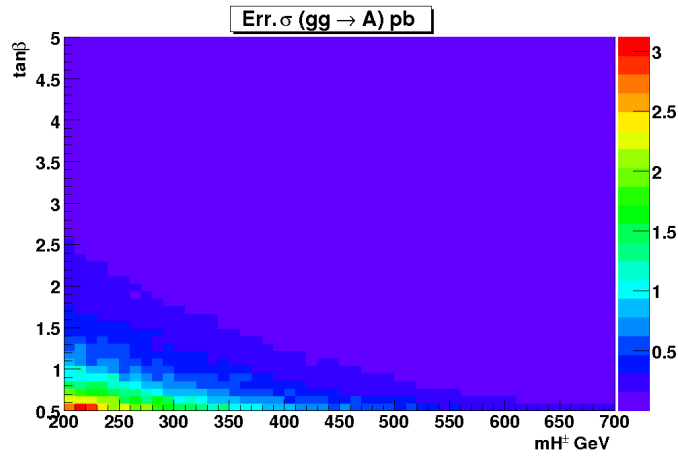
$$m_{H^\pm} = 340.0 \text{ GeV}, \quad \tan\beta = 2.50, \quad (21)$$

which yields, with the `2HDMC`, the following masses and widths:

$$\begin{aligned} m_{A^0} &= 486 \text{ GeV}, \quad m_{h^0} = 181 \text{ GeV}, \\ \Gamma_{A^0} &= 11.9 \text{ GeV}, \quad \Gamma_{h^0} = 0.563 \text{ GeV}, \quad \Gamma_{H^\pm} = 2.11 \text{ GeV}. \end{aligned} \quad (22)$$



(a) $\sigma(gg \rightarrow A^0)$ at pp 14 TeV in pb



(b) Error $\sigma(gg \rightarrow A^0)$ at pp 14 TeV in pb

Figure 9: *The Cross section and its error for $pp \rightarrow A^0$ at 14 TeV in the gg -channel.*

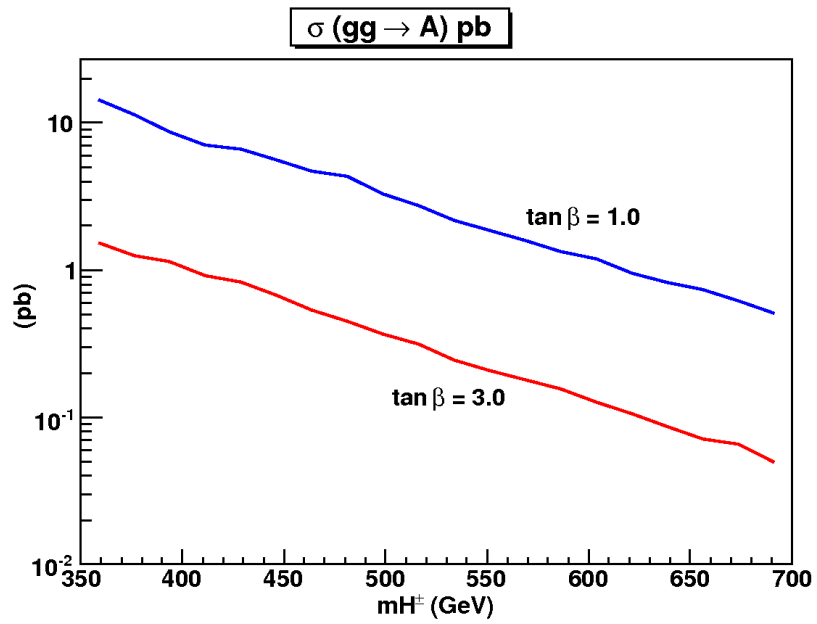


Figure 10: $\sigma(pp \rightarrow A^0)$ at 14 TeV in the gg -channel for $\tan \beta = 1.0$ and 3.0.

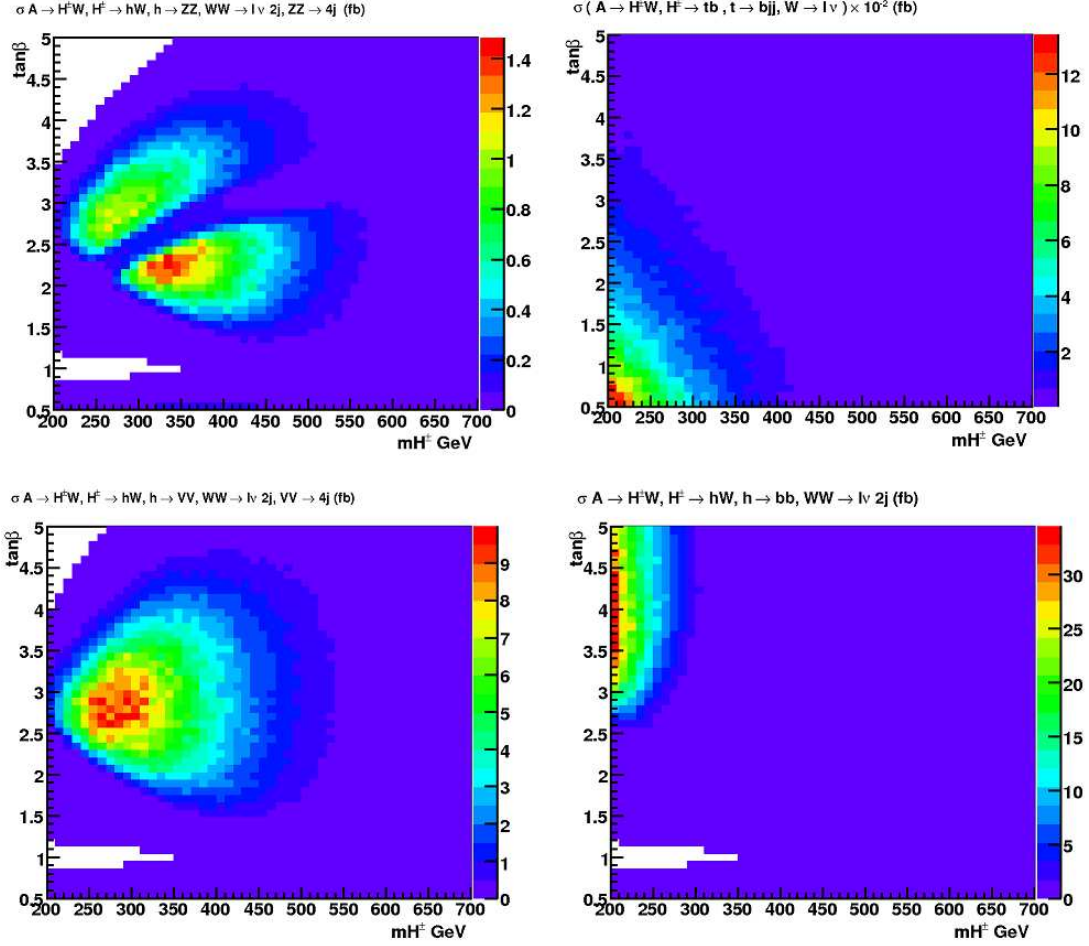


Figure 11: a) The upper left figure shows the total cross section for $A^0 \rightarrow H^\pm W^\mp$, $H^\pm \rightarrow h^0 W^\pm$, $h^0 \rightarrow ZZ$ where the Z 's decays hadronically and one W decays leptonically and the other one hadronically. We have fixed the origin of the W boson here so there is no combinatoric factor of 2 here. b) The lower left figure shows the same process but here $h^0 \rightarrow VV$, where $V \in [W, Z]$. c) The upper right figure is $H^\pm \rightarrow t\bar{b}/\bar{t}b$ where the top decays hadronically and the W boson leptonically. The cross section is given here in units of 100fb . d) The lower right figure shows the process $H^\pm \rightarrow h^0 W^\pm$, $h^0 \rightarrow bb$ whereof the W decays leptonically and the other one hadronically. Also in this case we have fixed the the W boson origin. ($\ell = e, \mu$)

The signal is generated in `Pythia`, with modified decay tables for the particles under investigation. As an example, this is how we tell `Pythia` to decay A^0 into $H^\pm W^\mp$:

```
36:oneChannel = 0 0.000844 101 21 21
36:addChannel = 1 0.5 101 24 -37
36:addChannel = 1 0.5 101 -24 37
```

The first line tells `Pythia` that particle with `id=36`, i.e. the A^0 according to PDG Monte Carlo numbering codes, to have a channel which is turned off, evaluated with matrix element method number 101, which results in two particles with `id=21` (gluons). This line is needed to be able to generate the A^0 in gluon fusion. The other lines specify $H^+ W^-$ and $H^- W^+$, turned on, with equal probability. The identity code is negated for antiparticles, thus `id=37` is the H^+ and `id=-37` is the H^- . By inspecting figure 11(c), we see that the total cross section is 6-7fb. A `Pythia` script generates the process, generates parton showering and hadronization and jet-finding with $\Delta R = 0,4$. For each event a `ROOT` tree-structure (`TTree`) is filled with the relevant four-vector components and some other interesting variables, such as the transverse mass for the $\ell\nu$ -pair, see section 3.5.2.

The background for this process is $pp \rightarrow t\bar{t}2j$, where j is either a gluon or a quark. A Les Houches file with 100k events are available in the LHC process library on the `MadGraph/MadEvent` homepage. The total cross section for the phase space region for this file is 660pb⁸. This file is fed into a `Pythia` script which then performs the same actions as the signal generating script.

3.5.2 Analysis

The whole analysis is divided into three levels/scripts. The first level was described above, where the raw events are generated, with some minor cuts. As example only those events which have *exactly* one charged lepton with $E_T > 10$ GeV are saved into the tree. This cut has barely any effect on the generated signal events, but has a considerable impact on the background, only 37% of the background events passes this cut. The trees generated at this first stage is then sent to an analysis-script.

The analysis-script performs the reconstruction of the Higgs-bosons. Since the invariant mass is a Lorentz invariant, we can separate events such that they have the correct intermediate resonances. The method used in this analysis depends on the two cases and will be explained later. As an example we look if four jets can combine into an invariant mass equal to the h^0 mass (± 50 GeV), with the constraint that these four jets can be divided into two pairs of jets which makes up an invariant mass of a vector boson (± 25 GeV).

Since we can not measure experimentally the longitudinal momentum component of the neutrino, the $W \rightarrow \ell\nu$ event can not be fully reconstructed. However, we can calculate a quantity called the *transverse mass* of the W boson [18]. The neutrino is detected by

⁸The boundaries on the phase space can be found at http://madgraph.phys.ucl.ac.be/MadGraphData/julien.caudron@fynu.ucl.ac.be/PROC2/Events/run_01_banner.txt

counting the total momentum and energy missing and assign those to the neutrino, we have:

$$\vec{p}_T = -\sum \vec{p}_T(\text{obs.}) \quad \cancel{E}_T = E_\nu, \quad (23)$$

where the slashed letter represents a *missing* quantity, thus only p_x, p_y are available. The transverse mass of a system of a neutrino and a lepton is given by:

$$m_{e\nu T}^2 = (E_{eT} + E_{\nu T})^2 - (\vec{p}_{eT} + \vec{p}_{\nu T})^2 \approx 2E_{eT}\cancel{E}_T(1 - \cos\phi_{e\nu}), \quad (24)$$

where $\phi_{e\nu}$ is the azimuthal angle between the electron and the neutrino. The transverse mass distribution for a W -boson going to $\ell\nu$ may look like figure 12. In the ideal case, no momentum- and energy smearing, the distribution would end at $m_W = 80.4$ GeV. Using

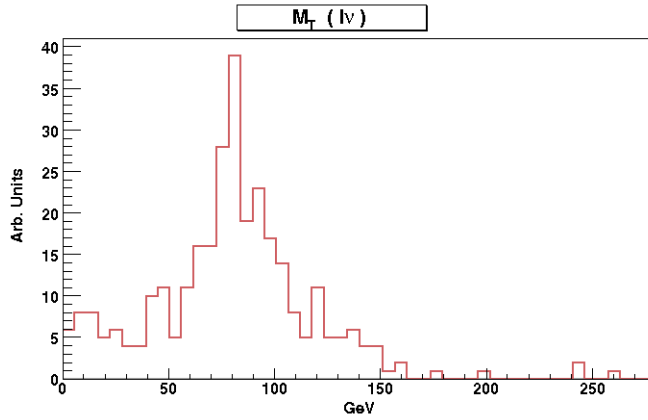


Figure 12: The m_T distribution for the $\ell\nu$ -pair from the W -boson in $A^0 \rightarrow H^\pm W^\mp$.

information on the transverse mass, we can postulate that the $\ell\nu$ -pair originated from a W if the pair has m_T within a certain range, say 50 to 100 GeV. We can then use the invariant mass relation to calculate the longitudinal momentum component ζ of the neutrino:

$$\begin{aligned} m_W^2 &= (80.4 \text{ GeV})^2 = (p_\ell^\mu + p_\nu^\mu)(p_{\ell\mu} + p_{\nu\mu}) \approx 2E_\ell E_\nu - 2\vec{p}_\ell \cdot \vec{p}_\nu \Rightarrow \\ m_W^2 &= 2E_\ell \sqrt{p_{x\nu}^2 + p_{y\nu}^2 + \zeta^2} - 2\vec{p}_{T\ell} \cdot \vec{p}_{T\nu} - 2\vec{p}_{L\ell} \cdot \zeta \Rightarrow \\ m_W^2 &= 2E_\ell \sqrt{p_{x\nu}^2 + p_{y\nu}^2 + \zeta^2} - 2p_{x\ell}p_{x\nu} - 2p_{y\ell}p_{y\nu} - 2p_{z\ell}\zeta \Rightarrow \\ \zeta &= -\frac{B}{2A} \pm \sqrt{\frac{B^2}{4A^2} - \frac{C}{A}}, \end{aligned} \quad (25)$$

where:

$$\begin{aligned} A &= 4(E_\ell^2 - p_{z\ell}^2), & B &= -4M p_{z\ell}, \\ C &= 4E_\ell^2(p_{x\nu}^2 + p_{y\nu}^2) - M^2 \\ M &= m_W^2 + 2p_{x\ell}p_{x\nu} + 2p_{y\ell}p_{y\nu}. \end{aligned}$$

We can not a priori know which sign in eq.(25) to pick. However, we know what the generated neutrino has as longitudinal momentum component and we can compare the two solutions with the true one. It is found that choosing the positive solution one obtains the best fit to the generated one. However, the difference is marginal - mean 16.6 vs. 20.1 for 496 events

in $A^0 \rightarrow H^\pm W^\mp$, $W \rightarrow \ell \nu$, see figure 13. Since the equation above is using the *physical* mass of the W and the generated one in general differs from that value, the square root of eq. (25) does not always have a positive argument. We can see this in figure 13, where we compare the generated and the reconstructed $p_{z\nu}$, only $\sim 1/3$ of the events are close to zero.

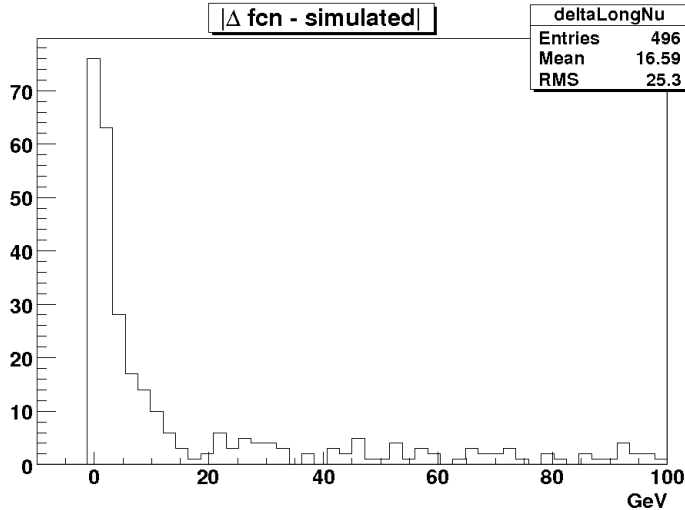


Figure 13: $|p_{L\nu}^{gen.} - \zeta|$ for the ν generated in the W -boson decay in $A^0 \rightarrow H^\pm W^\mp$. The mean value here is 16.6 GeV.

The last feature in the analysis-script is to provide the invariant mass spectrum of the charged Higgs, requiring that we have an intermediate h^0 -boson composed of intermediate V -bosons. Then we can also add a cut on either the invariant mass or the transverse mass for the H^\pm -associated W -boson. The relevant variables are then stored in another ROOT-tree and is sent to the third and last script, the plot-script. The plot-script draws a certain variable in the tree into as a histogram, over a subset of other tree-variables values using the ROOT TCut-class. Results and the different cuts we used will be given in the following sections for each process we considered.

3.5.3 Results 1

The first process we considered was $H^\pm \rightarrow 6j$, i.e. when the H^\pm -associated W -boson decays hadronically. The idea is to perform cuts on the various distributions for the signal and background simultaneously, keeping a maximum fraction of signal events and discarding a maximum fraction of background events. The signal cross section is around 6.5fb, and the background cross section is 660pb, i.e. $\sim 10^5$ times higher. We generated 953 signal events and 100k background events, so to obtain the same integrated luminosity⁹, we need to multiply the background events with a factor ~ 1000 . But this is in general not good, since

⁹ $N_{\text{events}} = \sigma \mathcal{L}$

there might be ONE event in the background for the H^\pm invariant mass - after multiplication should we expect 1000 background events there? We should provide the analysis with at least 10 times more background events, but since this will be very time- and memory consuming, we start investigating this relatively small background sample.

We show the distributions of ℓE_T , \cancel{E}_T , invariant mass of $4j$, invariant mass of $6j$, $m_T(\ell\nu)$ and invariant mass of $\ell+\nu+$ the hardest jet for the signal and background after the analysis-script in figure 14. The E_T -distributions for the 6 hardest jets for signal and background are shown in figures 15 and 16. After the analysis-script, we have lost about 66% of the signal events and rejected over 96% of the background. One should notice the difference on the m_T and ℓE_T distributions between signal and background. We can also see that the jet E_T -distributions are very similar. Also the η - and φ -distributions were investigated and no significant difference was noticed between signal and background.

In the plot-script, we employ the following cuts: $40 \text{ GeV} < m_T$, $\ell E_T < 130 \text{ GeV}$, $\cancel{E}_T < 300 \text{ GeV}$, invariant mass of $\ell+\nu+$ the hardest jet $< 370 \text{ GeV}$. The results are shown figure 17, where we have plotted the signal and background as a differential cross section of energy/mass; $d\sigma/dE$. The histograms are produced by multiplying them using the member function `Scale()` for ROOT histograms. The multiplication factor was $\sigma / (\text{Number of generated events} \times \text{Width of Bin})$. Thus, if we perform an integral over the energy variable, we obtain $f_{\text{cuts}} \times \sigma$, where $f_{\text{cuts}} = \text{Number of events passing cuts} / \text{number of generated events}$. The background is more than 3 orders of magnitude larger than the signal so the conclusion is that this signal is overwhelmed by the $t\bar{t}2j$ background.

3.5.4 Results 2

The second process we considered was $H^\pm \rightarrow \ell\nu 4j$, i.e. when the H^\pm -associated W -boson decays leptonically. The main-difference here comparing with the last section is that the m_{H^\pm} -peak is slightly more sharpened but we loose around 78% of the signal events already at this stage. The signal distributions are almost identical as in the previous section, so the conclusion is that neither this signal can be seen experimentally. The results will be summarized and further commented in chapter 4

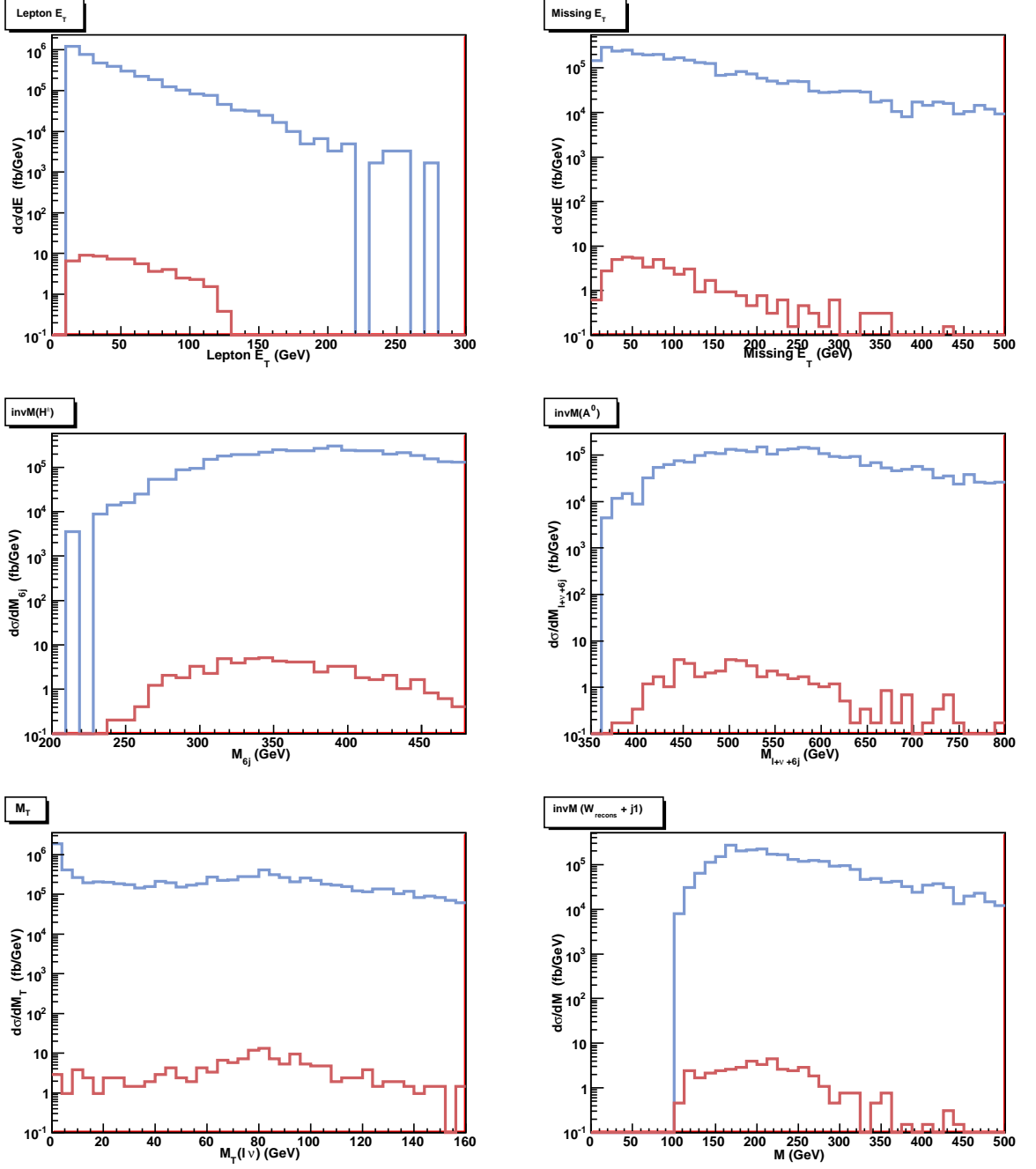


Figure 14: Background $pp \rightarrow t\bar{t}2j$ (blue) and signal $H^\pm \rightarrow 6j$ (red) after reconstruction of intermediate particles. a) The upper left figure is the ℓE_T -distribution. b) The upper right figure \cancel{E}_T . c) The middle left figure is the invariant mass distribution of $6j$. d) The middle right figure is the invariant mass of $\ell\nu_{recons.}6j$. e) The lower left figure is the transverse mass of $\ell\nu$. d) The lower right figure is the invariant mass distribution of $\ell\nu_{recons.}$ + the hardest jet.

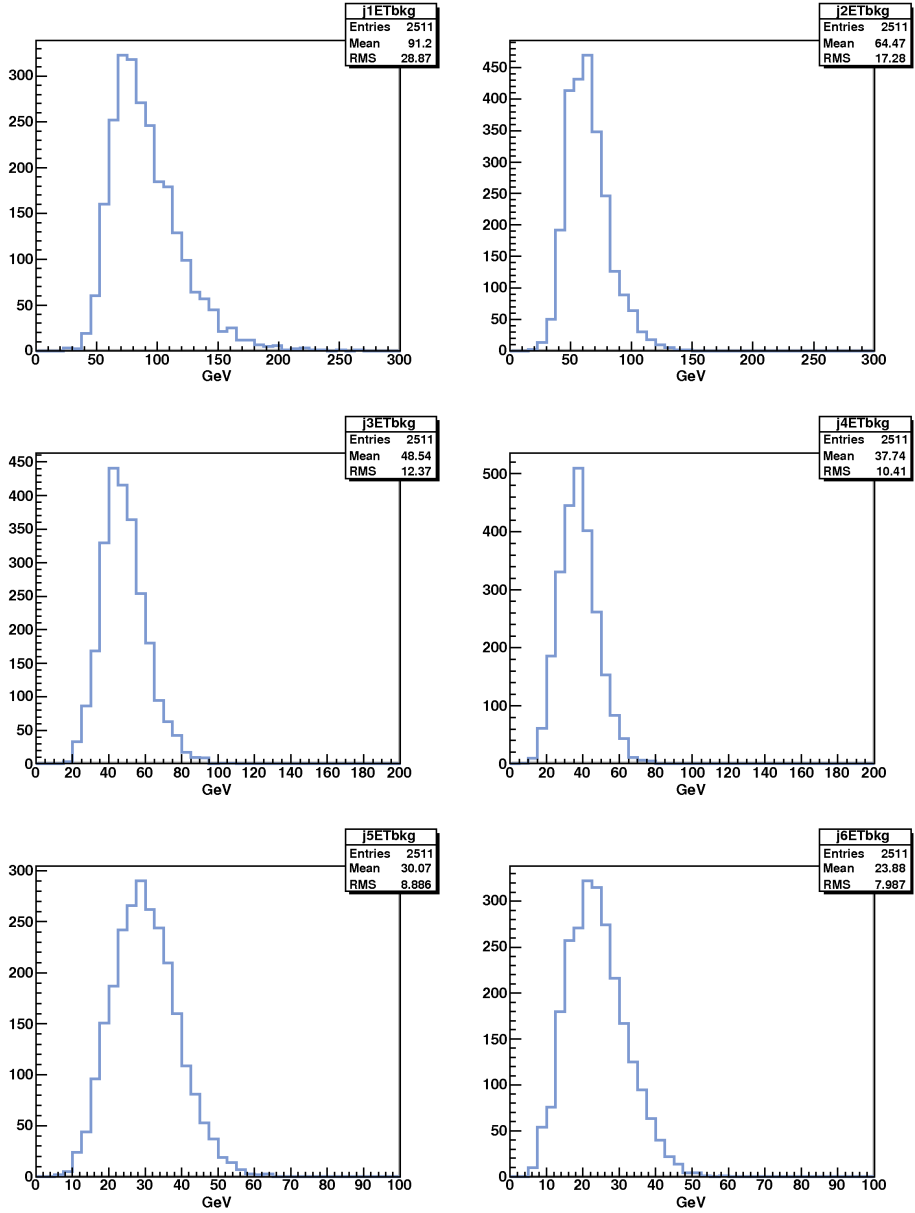


Figure 15: The E_T -distribution of the six hardest jet from the background reaction $pp \rightarrow t\bar{t}2j$. No particular normalization is employed, so that the y-axis is in arbitrary units.

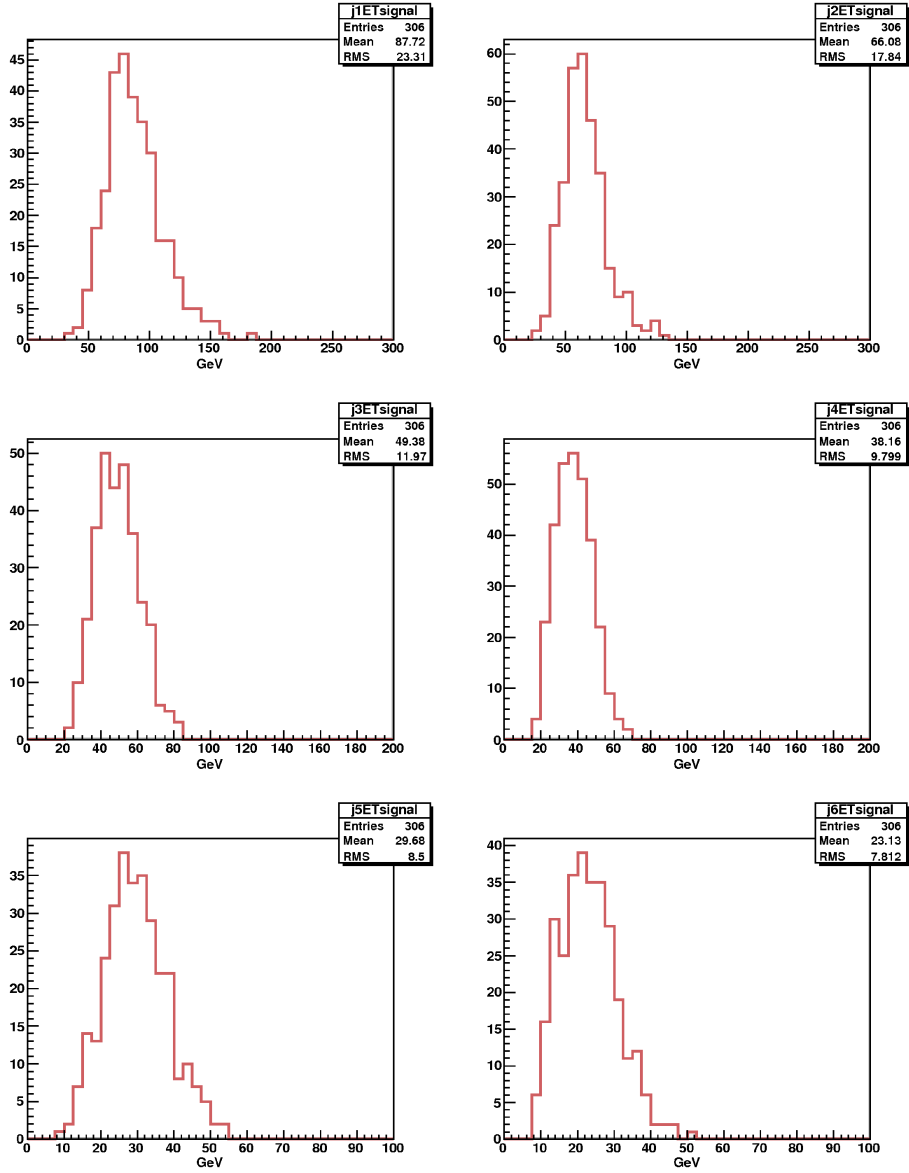


Figure 16: The E_T -distribution of the six hardest jet from the signal reaction $A^0 \rightarrow H^\pm W^\mp \rightarrow \ell \nu 6j$. No particular normalization is employed, so that the y-axis is in arbitrary units.

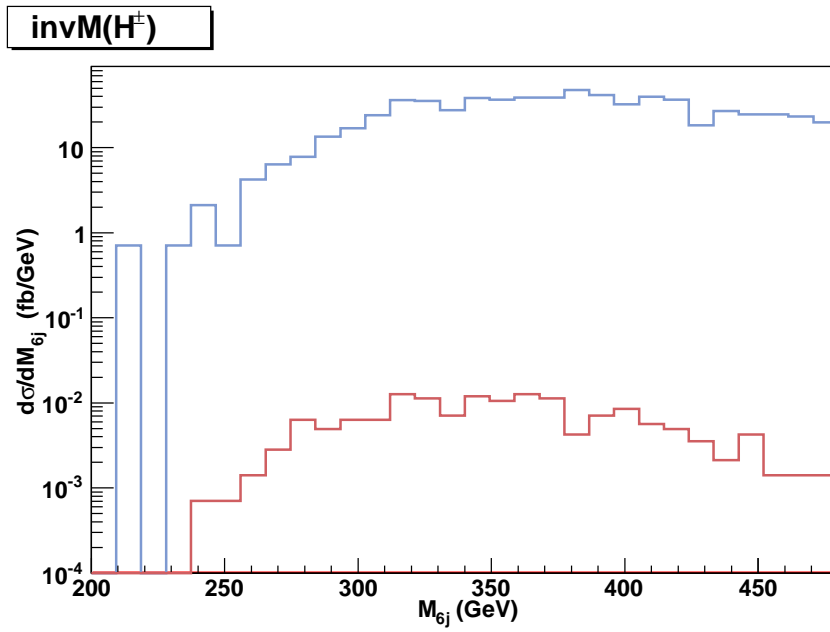


Figure 17: Invariant mass of 6 jets for background $pp \rightarrow t\bar{t}2j$ (blue) and signal $H^\pm \rightarrow 6j$ (red) after cuts: $40 \text{ GeV} < m_T$, $\ell E_T < 130 \text{ GeV}$, $\cancel{E}_T < 300 \text{ GeV}$, invariant mass of $\ell + \nu +$ the hardest jet $< 370 \text{ GeV}$.

3.6 The process $H^\pm \rightarrow t\bar{b}/\bar{t}b$

The final state $\ell\nu 4j$ resulting from $pp \rightarrow A^0 \rightarrow H^\pm W^\mp$, $H^\pm \rightarrow t\bar{b}/\bar{t}b$ has a significantly greater cross section than the process investigated in the last section. However, this process has not as many intermediate particles and we have to fight the devastating $t\bar{t}$ -background. We will simulate $H^\pm \rightarrow t\bar{b}/\bar{t}b$ again using `Pythia`, also $t\bar{t}$ will be generated with `Pythia`. We choose the point (260, 1.2) in $(m_{H^\pm} \tan\beta)$ -space where the total signal cross section is approximately 500 fb, figure 11 c. We simulate 1037 events with no distinction of the 2 possible W -decay configurations, thus the signal cross section is about 1pb. The cross section for the background $gg/q\bar{q} \rightarrow t\bar{t}$ is evaluated with `Pythia` resulting in 520pb. We generate 700k events of $t\bar{t}$, so in order to obtain the same integrated luminosity as the signal we need to scale the background with a factor 0.77. At this stage we want to plot the invariant mass of the 4 jets, with only a basic cut on the number of charged leptons with $E_T > 20$ GeV and transverse mass for the $\ell\nu$ pair in the range 50 to 250 GeV. But since we aim to proceed further with this decay channel of the charged Higgs, we have started to implement b -matching in our analysis, since we might want to use such information to make some cuts.

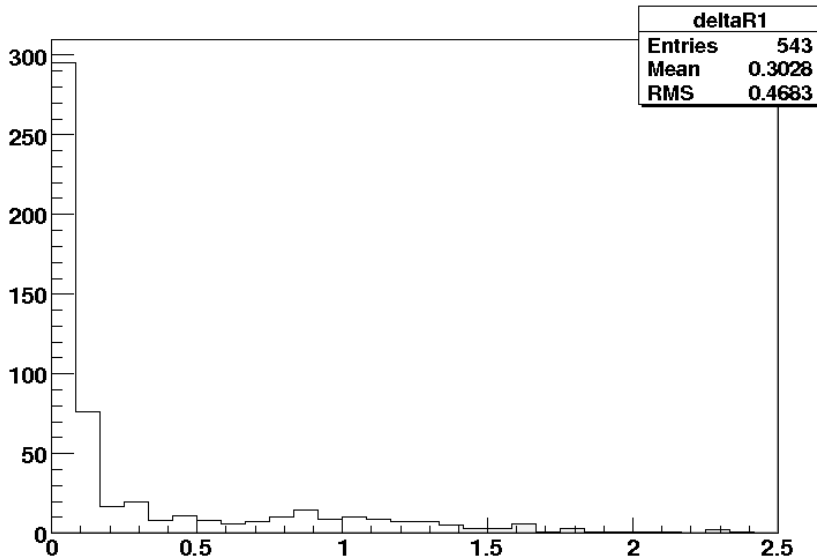


Figure 18: *The difference in η, φ -plane for one specific b -quark and the closest jet.*

In an experimental analysis, we can b -tag the jets resulting from a hard b -quark, by looking for displaced vertices in the central detector. Since we do not have such tools at hand - a detector simulation tool, we instead assign 100% b -tagging efficiency and perform a b -matching with our jets. At this stage, we search for among the four hardest jets and find which jet found by `CellJet` is closest to a generated b -quark in the (φ, η) -plane. We require that the b -quarks are in two distinctive jets and that the b -quark is within $\Delta R < 0.4$. This procedure has an efficiency of $\sim 80\%$, see figure 18, so the efficiency of double b -matching is $\sim 70\%$. The parameters for the jet-algorithm were $\Delta R = 0.4$ and $\min.E_T^{\text{jet}} = 30$ GeV. In

this procedure, we required at least 4 jets in the final state.

After the requirement of having exactly one charged lepton with $E_T > 20$ GeV we have reduced the signal with 25% and the $t\bar{t}$ -background with 64%. The requirement of double b -matching and at least 4 final state jets, further reduced the signal and the background with 61% and 65% respectively. After these cuts, we save the relevant four-vectors into ROOT trees and proceed further using a ROOT script similar to the “plotting script” in the last section. As mentioned earlier, we plot the invariant mass distribution of the 4 jets with a cut on the transverse mass of the $\ell\nu$ pair being in the range $50 < m_{T\ell\nu} < 250$ GeV. At this stage, there is no significant difference between signal and background in their m_T -distributions the lepton-, missing- and jets E_T - and all η - and φ - distributions. The invariant mass distribution for the sum of 4 jets is shown in figure 19.

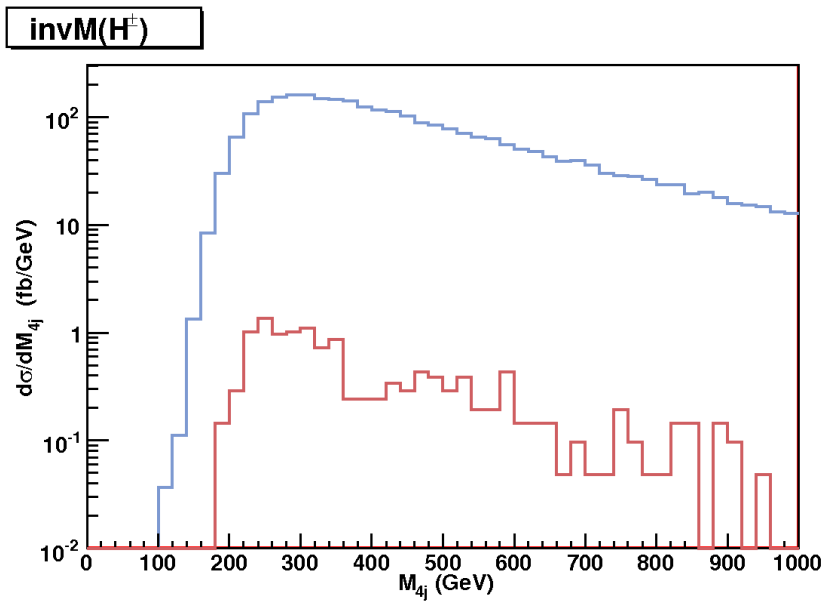


Figure 19: *Invariant mass distribution for the 4 jets in $H^\pm \rightarrow t\bar{b}/\bar{t}b$ signal (red) and $t\bar{t}$ -background (blue).*

There is a study of $W^\pm H^\mp$ at the LHC within the MSSM by [19] where one considered this production *without* an intermediate A^0 resonance. They considered the same decay of the charged higgs and the $2W$ bosons, with a total event rate $10^{-4} - 10^{-3}$ to the $t\bar{t}$ -background. Their analysis was completely partonic and assumed 100% b -tagging efficiency. Their results are that for charged Higgs masses below 500 GeV, the background from $t\bar{t}$ is approximately 10 times bigger in their case, see figure 20.

4 Discussion and future prospects

The results from the 2HDMC together with cross sections from PYTHIA clearly disfavour the charged Higgs to be detected via the gold-plated $h^0 \rightarrow 4\ell$. To obtain the cross section for this channel, we first convert the $ZZ \rightarrow 4j$ in figure 11 a) into $ZZ \rightarrow 4\ell$ by dividing with

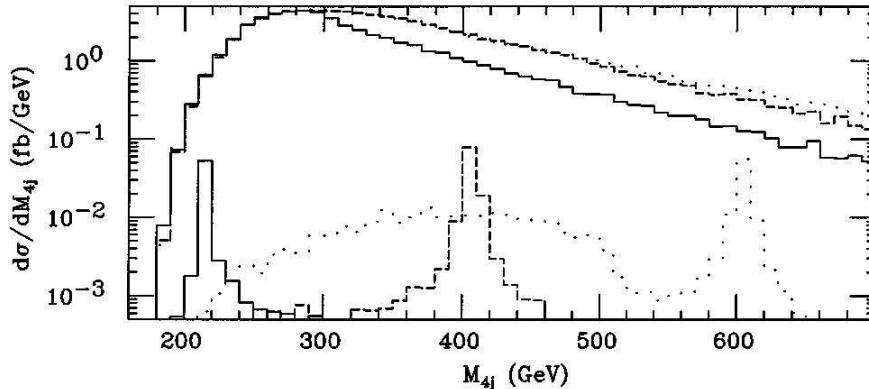


Figure 20: *Invariant mass distribution for the 4 jets in $H^\pm \rightarrow t\bar{b} / \bar{t}b$ and $t\bar{t}$ -background from [19]. The masses of the generated charged Higgs are 214, 407 and 605 GeV.*

100, since $\mathcal{B}(Z \rightarrow \ell\ell) = 0.1 \times \mathcal{B}(Z \rightarrow jj)$. Then we convert the $W \rightarrow \ell\nu$ into $W \rightarrow 2j$ by multiplying with 3. Thus, the maximum cross section for this channel is only $\sim 0.05\text{fb}$.

In this thesis we first examined the $A^0 \rightarrow H^\pm W^\mp$, $H^\pm \rightarrow h^0 W^\pm$, $h^0 \rightarrow VV$, $VV \rightarrow 4j$. We avoid the $t\bar{t}$ background, but we have to fight the $t\bar{t}2j$ background. Even though we have many intermediate particles in the signal, we can not reduce the background to the desired level. What can be improved is perhaps to use a better cone-based jet algorithm, and use separation in the (φ, η) -plane between particles as cuts. But this can most likely not reduce the $t\bar{t}2j$ background with a factor $\sim 10^3$ which is needed.

In the case of $H^\pm \rightarrow t\bar{b} / \bar{t}b$, we have a better starting point, the signal cross section is “only” 10^{-3} times the $t\bar{t}$. But we do not have many cuts related to reconstruction of intermediate particles to play with here so the background to signal ratio for 4 jet-invariant mass is around 100 to 1. However, there is hope that one can find cuts by comparing invariant masses of various combinations of jets and the lepton as one did in [19]. We would perhaps also like to find a good transverse quantity for the entire $\ell\nu 4j$ final state, and imposing a cut there by assuming that the mass of the A^0 is known prior to the analysis. We could also try to perform analyses on more points in the $(m_{H^\pm}, \tan\beta)$ - space.

One should also take note of the shape of the signal distributions in figure 20, the peak is around 2 orders of magnitude high and is contained in one single bin. Translating this to a linear scale, the distribution should become very sharp peaked. This is clearly a feature of their partonic approach. In a more realistic study, such as the one we performed in this thesis, the distribution of $m(4j)$ will become much broader for the signal. This will also affect the background, but in this case the effect is much smaller due to the flatness of $m(4j)$ from $t\bar{t}$.

Finally, since the LHC will basically be a “top-factory”, and $t\bar{t}$ is one of the most prominent backgrounds for many interesting signals for physics beyond the standard model, one will study and learn more about the features of $t\bar{t}$. Thus, one should try to gain further insight in how $t\bar{t}$ will be realized in experimental analyses once LHC starts up.

Acknowledgements

The author would like to thank all members in Uppsala THEP group: Oscar for all technical aid and interesting physics chats, Johan for great company during Lund Monte Carlo School and proof reading drafts of this thesis, Gunnar for being a great source of inspiration. Finally the author would like to thank Rikard, for all help and guidance during this project.

References

- [1] M. Peskin & D. Schroeder *An Introduction to Quantum Field Theory*, Westview Press 1995
- [2] B. Povh *Particles and Nuclei 5th ed.*, Springer 2006
- [3] *Limits on Massless Particles*, Phys. Lett. B96 p. 56, Weinerg & Witten
- [4] *REVIEW OF PARTICLE PHYSICS*, Particle Data Group 2008
- [5] I. Aitchison *Supersymmetry in Particle Physics*, Cambridge 2007
- [6] C. Grupen *Astroparticle Physics*, Springer 2005
- [7] J. Ellis *Supersymmetry for Alp hikers*, arXiv:hep-ph/0203114v1
- [8] M. Srednicki *Quantum Field Theory*, Cambridge 2007
- [9] A. Pich *The Standard Model of Electroweak Interactions*, arXiv:0705.4264v1 [hep-ph]
- [10] S. F. Novaes *Standard Model: An Introduction*, arXiv:hep-ph/0001283v1
- [11] D.J. Miller et. al. *The Higgs Sector of the Next-to-Minimal Supersymmetric Standard Model*, arXiv:hep-ph/0304049v2
- [12] R. Barbieri et. al. *Supersymmetry without a light Higgs boson*, Phys. Rev. D **75**, 035007 (2007)
- [13] L. Cavicchia et. al. *Supersymmetry without a light Higgs boson at the CERN LHC*, Phys. Rev. D **77**, 055006 (2008)
- [14] <http://www.isv.uu.se/thepp/MC/2HDMC/>
- [15] *PYTHIA 6.4* <http://home.thep.lu.se/~torbjorn/pythia/lutp0613man2.pdf>
- [16] *PYTHIA 8.1* <http://home.thep.lu.se/~torbjorn/pythia8/pythia8100.pdf>
- [17] <http://madgraph.hep.uiuc.edu/>
- [18] T. Han *Collider Phenomenology*, arXiv:hep-ph/0508097v1
- [19] S. Moretti and K. Odagiri, *Phenomenology of $W^\pm H^\mp$ production at the CERN Large Hadron Collider*, Phys. Rev. D **59**, 055008 (1999)